



UNITED NATIONS
UNIVERSITY

UNU-GTP

Geothermal Training Programme

Orkustofnun, Grensasvegur 9,
IS-108 Reykjavik, Iceland

Reports 2016
Number 41

MODELLING OF TRACER TESTS IN A GEOTHERMAL RESERVOIR IN TIANJIN, CHINA

Wang Wanli

Institute of Hydrogeology and Environmental Geology - IHEG
268 North Zhonghua Street, Shijiazhuang
050061, Hebei Province
P.R. CHINA
Wanliwang2010@163.com

ABSTRACT

The Wumishan (Jxw) geothermal reservoir in the Dongli Lake area is an extensive, low-temperature geothermal system hosted mainly by Mesoproterozoic dolomitic limestone. In order to study the flow paths and predict the cooling due to long term injection, tracer tests were performed on the 17th of December, 2015. 700 kg of Ammonium Molybdate (Mo) were injected into well DL-48B. No obvious tracer recovery was detected in the water samples collected during the 90 days of tracer test. In order to interpret the tracer testing quantitatively, both an analytical method developed by ISOR (Iceland GeoSurvey) and a numerical method using Visual MODFLOW flex software were applied. For the analytical model, it was assumed that the recovery is very slow and would appear after 90 days. In the three cases of longitudinal dispersivity, 77, 230 and 384 m, the tracer concentration began to increase after 150 days. When the dispersivity was 77 m, thermal breakthrough would occur in 80 years for a narrow flow channel scenario and 27 years for a wide flow channel scenario with an average annual production and injection rate of 10 kg/s. Using an automatic parameter estimation tool along with the numerical model, errors were minimized between the observed and the simulated data to estimate the distribution of the reservoir parameters. There is reasonable agreement between the simulated and observed water levels and therefore the numerical model was used to predict the tracer concentration in the production well. For the most pessimistic case (longitudinal dispersivity of 384 m), the tracer will take more than a year to arrive at the production well with concentration values outside of the detection limit, according to the model. Results show that there is no direct connection between production and injection wells and neither of the models predicts cooling in the next 24 years.

1. INTRODUCTION

Geothermal reinjection is important in geothermal reservoir management because it helps maintain reservoir pressure. It has become an integral part of sustainable and environmentally friendly geothermal utilization projects. However, it poses the possible danger of cooling production wells (Axelsson, 2012a). An optimum reinjection strategy should balance the requirements of sustaining the reservoir pressure and preventing early thermal breakthrough of reinjected water (Diaz et al., 2016).

Tracer testing has been widely used and proved to be an important and useful tool in studying the impact of reinjection (Axelsson et al., 2005; Mondejar, 2012; Koech, 2014; Pang, 2010). In conventional geothermal development, tracer testing can provide information on the flow-paths between injection and production wells and help predicting the danger and rate of cooling of the production wells during long-term reinjection (Axelsson, 2013).

Most tracer test interpretations are only used in a qualitative manner to assess injector-producer connectivity without taking advantage of other information carried within a full tracer response curve (Alramadhan et al., 2015). To interpret the tracer testing quantitatively, both an analytical method developed by ISOR (Iceland GeoSurvey) and a numerical method using Visual MODFLOW flex software were applied. The results are described in this report.

The study area, Dongli Lake, is located in Tianjin Binhai New District with an area of 62 km² (Figure 1). This area is rich in low-temperature geothermal resources, which are stored in sedimentary reservoirs consisting mostly of Mesoproterozoic dolomitic limestone (Duan et al., 2011). Geothermal wells are mostly located in the regional structural high, known as the Cangxian uplift (Minissale et al., 2008). The geothermal water is mainly used for space heating during winter and also for bathing and agriculture (Axelsson and Dong, 1998).

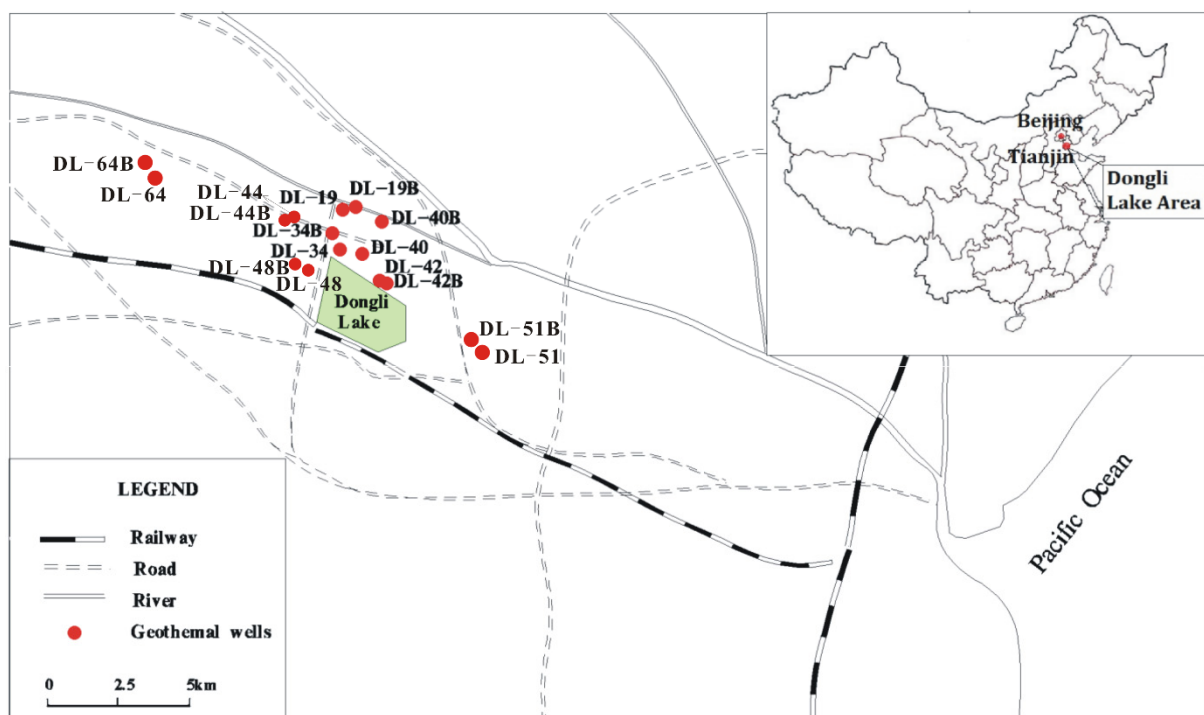


FIGURE 1: Map of the study area (modified after Zhao, 2010)

Due to gradually increased production and development, the water level has been falling 6-9 m per year since 1997 and a regional cone of depression has formed (Cheng et al., 2010). Therefore, in order to maintain reservoir pressure and prolong the lifetime of the production wells, reinjection of the used geothermal water started in 2001 (Duan et al., 2011). Reinjection provides an additional recharge to geothermal reservoirs. However, the water level has still been dropping nearly 3 m per year since 2011 due to large scale development (Ruan et al., 2015).

In order to study the flow paths and predict the cooling of long term injection, tracer testing was performed. The test started on December 17, 2015, with 700 kg of Ammonium Molybdate (Mo) injected

into the injection well DL-48B (Figure 1). Water samples were collected from eight production wells within a 3.3 km radius from the injection well for up to 3 months.

In this project, the aim is to model the flow patterns and predict the cooling time in the geothermal reservoir. Since no tracer was detected in the samples, tracer recovery was simulated and predicted based on several assumptions for the analytical method. Furthermore, a numerical model was built in order to demonstrate physical processes in the study area, and predict the change of concentration over a long time period after tracer injection.

2. THE GEOTHERMAL FIELD

2.1 Geological setting of the study area

The geothermal reservoir in Tianjin can be divided into a porous part and a bedrock part (An et al., 2016) (Figure 2). According to borehole data (Tian, 2014), the porous geothermal reservoir consists of continental sediments (Cenozoic Mesozoic Minghuazhen Group (Nm) and Guantao Group (Ng)) and their permeability is dominated by primary porosity. The Karstic-fracture geothermal reservoir (Paleozoic Ordovician (O), Cambrian (ϵ) and Mesoproterozoic Jixian Wumishan Group (Jxw)), is up to 6000 m thick with fracture-dominated secondary permeability (Minissale et al., 2008).

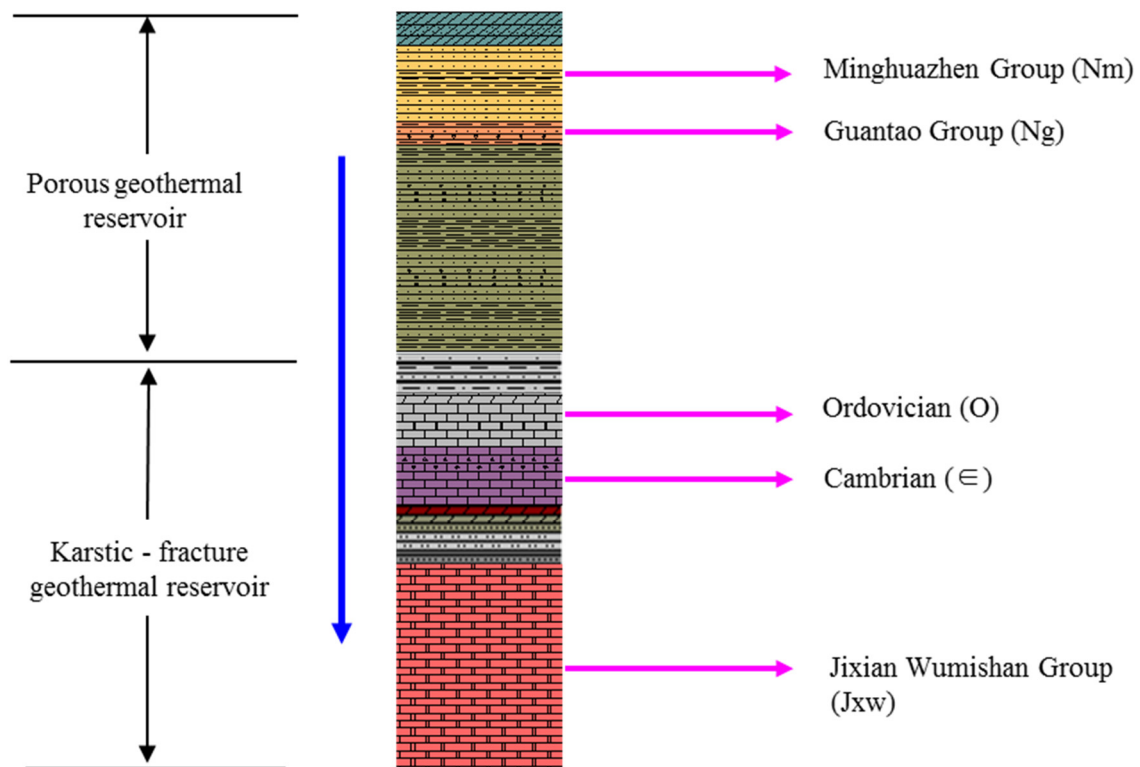


FIGURE 2: Geologic setting of the main geothermal reservoir

The Tianjin reservoir is bounded by the Tianjin fault in the west, by the Haihe fault in the south, and by the Hangu fault in the north (Zhao, 2010) (Figure 3). The most important one is the Cangdong fault, which crosses the study area and has a great impact on both the strata and heat (Figure 3). The Wumishan formation lies at a much shallower depth in the west of the Cangdong fault than in the east side of the fault. Near the fault, the strata has high permeability and conductivity.

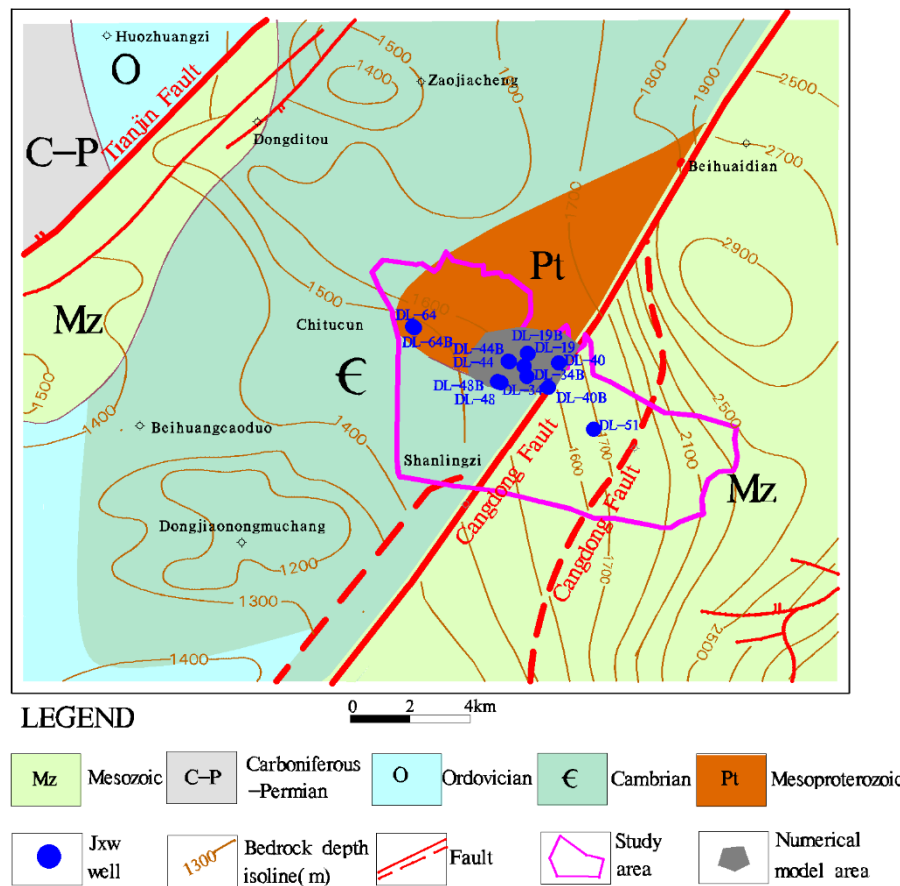


FIGURE 3: Geological formations and structures of the study area

2.2 The geothermal reservoir – Jxw

The Wumishan geothermal reservoir (Jxw) is the area of study in this project. It mostly consists of Mesoproterozoic dolomitic limestones (Duan et al., 2011). Therefore, the reservoir has good karst features, i.e. high temperature and high production rates (Zhao, 2010). From the previous study in this area, it is known that the fracture rate of this reservoir varies from 40 to 70% and in some wells, the rate is up to 80-90% (Lin, 2006).

The Quaternary and Tertiary formations consist of clay and sandstone, forming a good caprock of the geothermal reservoir. They are of low thermal conductivity and low permeability with thickness of 280-320 m. The Cangdong fault is a major fault in this area which can conduct heat from the bottom of the reservoir to the shallow part by heat convection. Heat convection becomes weaker with increasing distance from the fault (Zhao, 2010). The heat source of the reservoir is presumably an upper mantle heat-flow anomaly and radioactive decay from granite (8-16 km depth). According to isotopic analysis, the origin of the water in the reservoir is meteoric from ancient times.

Geothermal wells are mostly located near the Cangdong fault (Figure 3). Thirteen geothermal wells have been drilled into the reservoir (see Table 1). Average well production rates are in the range of 70-120 m³/h, with wellhead temperatures between 88 and 102°C (Fan, 2006; Tian, 2014). However, no well completely penetrates the reservoir and its thickness is unknown. Drilling data shows that west of the Cangdong fault, the top depth of the reservoir varies from 1752 to 2016 m, with a thickness of 480 to 1032 m. However, on the east side of the fault, only well DL-51 penetrates the reservoir, here the depth to the top is 3581 m and the thickness 153 m.

TABLE 1: Details of geothermal wells in the Dongli Lake area (Jxw) (Tian, 2014)

Well	Reservoir	Depth (m)	Temperature at wellhead (°C)	Max flow rate (m ³ /h)	Thickness of the reservoir (m)
DL-44	Jxw	2373.14	98	112.78	462
DL-44B	Jxw	2495	98	112.78	468
DL-34	Jxw	2327.1	100	204.61	
DL-34B	Jxw		96.5	140 [*]	
DL-19	Jxw	1842	83	49.2	
DL-19B	Jxw	2384.36	88	117.98	
DL-40	Jxw	2328.01	98.5	126.04	534
DL-40B	Jxw	2278.99	101	126.04	509
DL-51	Jxw	3634	97	70.71	153
DL-48	Jxw	2328.7	93	121.97	374
DL-48B	Jxw	2533.7	93	112.78	671
DL-64	Jxw	2564.6	93	126	798.6
DL-64B	Jxw	2783.81	96	119	1031.81

* Zhao (2010)

The water types in the study area of the Wumishan formation thermal reservoir are mainly $\text{HCO}_3 \cdot \text{Cl} \cdot \text{SO}_4 \cdot \text{Na}$ and $\text{HCO}_3 \cdot \text{Cl} \cdot \text{Na}$, and the mineralization degree is 1600-2200 mg/L. The further the distance is to the Cangdong fault, the higher mineralization degree is observed in the geothermal wells (Ruan et al., 2015).

2.3 Reservoir temperature

Reservoir temperature analysis is based on data from injection well DL-48B. Figure 4 shows the warm-up temperature logs of well DL-48B. It is assumed that the well had reached thermal equilibrium in November 2015, hence the profile measured on November 2015 should reflect the true formation temperature.

Formation temperature increases gradually from the surface to about 1875 m depth, this indicates that conduction is the dominant heat transfer process within the formation. The top of the Jxw reservoir and the main feed zone seems to be intersected, as a fast increase of temperature indicates, reaching the maximum of 99.92°C at 1900 m depth. At greater depth, a temperature reversal is observed, most likely associated with the development of fissures in the well causing cold water to enter. Considering other wells nearby, the temperature stays constant when the depth increases, which indicates that convection dominates heat transfer in this formation, not conduction.

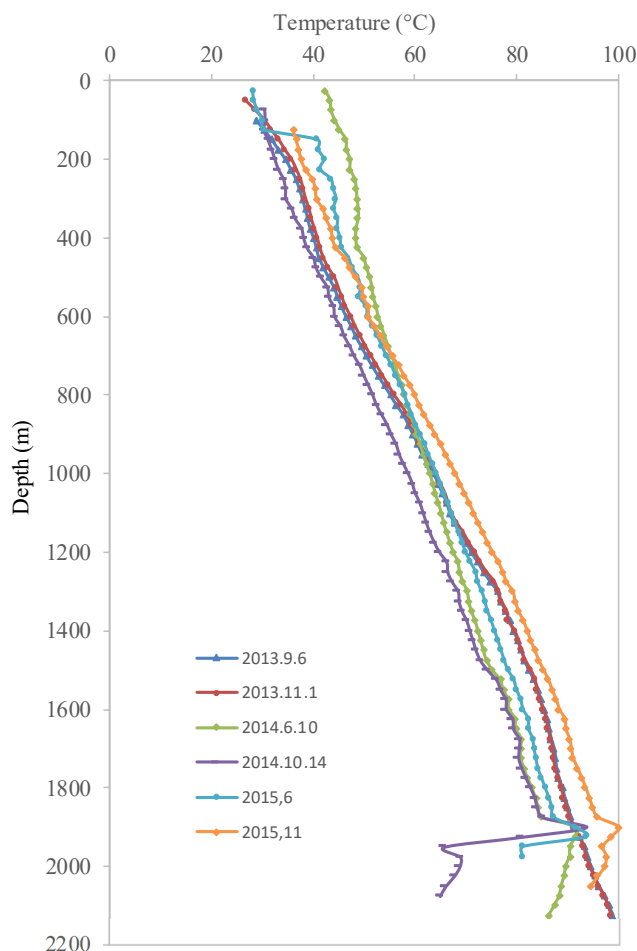


FIGURE 4: Warm-up temperature profiles from injection well DL-48B

2.4 Production in the study area

The exploration of the geothermal resources in the Dongli Lake area started in the 1980s (Zhao, 2010). With the increasing water demand for space heating and domestic water supply, the total production and the number of wells gradually increased.

Currently, there are 22 geothermal wells in this area, including 13 wells in the Wumishan geothermal formation – 7 production and 6 injection wells. In 2008 and 2009, the total annual production and injection were only $59.4 \times 10^4 \text{ m}^3$ and $53.4 \times 10^4 \text{ m}^3$, respectively (Zhao, 2010). In 2012, the total production rapidly increased and reached $140.7 \times 10^4 \text{ m}^3$ (Ruan et al., 2015). In 2013, the production increased to $157.4 \times 10^4 \text{ m}^3$, with a slight decrease in the production in 2014, to $147.0 \times 10^4 \text{ m}^3$.

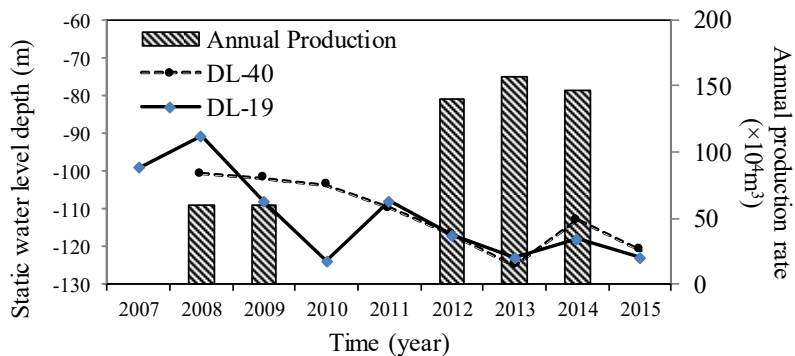


FIGURE 5: Static water level depth and annual production rate from 2007 to 2015

production rate from 2007 to 2015. Most of the production wells were shut off after the domestic heating period, from 15th November until 15th March, so the water level fluctuates significantly between seasons.

Due to intensive development and continuous increase in production, the water level has gradually declined in the reservoir. According to the dynamic monitoring data from 2012, the water level in the Jxw reservoir was at about 110 m below the surface, while in 2015 it was at around 120 m depth. Hence, the annual decline is about 3 m/year (Ruan et al., 2015). Figure 5 shows the static water level and corresponding

3. TRACER TESTING

Before starting a tracer test, the proper tracer has to be chosen. The tracer needs to meet a few basic criteria, such as:

- Not be present in the reservoir or at a concentration much lower than the expected tracer concentration;
- Not react with or be absorbed by reservoir rocks;
- Be thermally stable at reservoir conditions;
- Be relatively inexpensive;
- Be easy (fast/inexpensive) to analyse;
- Be environmentally benign (Axelsson, 2013); and
- The tracer should be detectable at low concentrations (Nottebohm et al., 2012).

Ammonium Molybdate (Mo) was used for the tracer test. It is nontoxic at low concentrations and could be used safely in the aquifer. The natural concentration of the tracer was low (background concentration is around $0.5 \mu\text{g/L}$) so it was assumed that the tracers introduced for this test could be followed over a reasonable distance and still be detected (Leblanc et al., 1991).

On December 17, 2015, 700 kg of Ammonium Molybdate were injected into well DL-48B over a period of 2 hours (Figure 3). The injection flow rate was approximately $100 \text{ m}^3/\text{h}$. Then, eight production wells were sampled every 2 hours throughout the subsequent 3 months (Figure 3). Only 1/6 of the samples were tested and analysed. If the tracer had been detected, the frequency of the analysis could have been increased.

No recovery was detected in the samples after 90 days of sampling which took place until March 18, 2016. There are a couple of possible explanations. One is that the tracer needs longer time to arrive at the production wells. Another possibility is that there is no direct flow from the injection well to production wells as the reservoir is highly fractured.

3.1 Simulation of tracer recovery and interpretation

3.1.1 Basic theory of tracer transport

The theory of tracer transport is the same as solute transport in porous and fractured hydrological systems. The principal models include transport by advection and convection, mechanical dispersion and molecular diffusion (Axelsson et al., 2005).

Various analytical models and solutions have been developed to interpret tracer test data after highly simplifying the geometry, dispersion, etc. The simple one-dimensional flow-channel tracer transport model is a rather powerful tool (Axelsson et al., 2005). This model assumes that the flow between injection and production wells can be approximated by one-dimensional flow and flow channels could be parts of near-vertical fracture-zones or parts of horizontal interbeds or layers. This one-dimensional tracer transport model is governed by the following equation (Axelsson et al., 2005):

$$D \frac{\partial^2 C}{\partial x^2} = \mu \frac{\partial C}{\partial x} + \frac{\partial C}{\partial t} \quad (1)$$

where D is the dispersion coefficient (m^2/s), C is the tracer concentration in the flow-channel (kg/m^3), x is the distance along the flow channel (m), μ is the average fluid velocity in the channel (m/s) and t is the time (s). Furthermore, $\mu = q/\rho A\phi$, where q is the injection rate (kg/s), ρ is the water density (kg/m^3), A is the average cross-sectional area of the flow-channel (m^2) and ϕ is the flow-channel porosity.

Molecular diffusion is neglected in this simple model so that $D = \alpha_L \mu$, where α_L is the longitudinal dispersivity of the channel (m).

Assuming instantaneous injection of a mass M (kg) of tracer at time $t=0$, the solution is given by:

$$c(t) = \frac{\mu M \rho}{Q} \frac{1}{2\sqrt{\pi D t}} e^{-(x-\mu t)^2/4Dt} \quad (2)$$

where $c(t)$ is the tracer concentration in the production well fluid (kg/m^3) and Q the production rate (kg/s). Conservation of the tracer according to $c \times Q = C \times q$ has been assumed.

Considering that the initial (background) tracer concentration of the production well fluid is not always 0, Equation 2 can be revised as follows:

$$c(t) = \frac{\mu M \rho}{Q} \frac{1}{2\sqrt{\pi D t}} e^{-(x-\mu t)^2/4Dt} + c(0) \quad (3)$$

3.1.2 Assumptions and simulation

This report will focus on data from injection well DL-48B and nearby production well DL-48 (Figure 3). Even though no tracer recovery was detected in the water samples during the 90 days' tracer test, it can be assumed that the recovery is very slow and if sampling had been continued, recovery would have appeared later. For assessing possible flow-paths between production and injection wells and predicting the cooling time, three assumptions are made for injection well DL-48B and production well DL-48:

1. Based on the sampling, tracer concentration is similar to the background concentration during the 90 days period. So we assume that from $t=\text{day } 1$ to $t=\text{day } 90$, the concentration is $0.5 \mu\text{g}/\text{L}$.

2. According to tracer tests from other geothermal fields, the value of dispersivity α_L is usually between $0.1x$ and $0.5x$ (where x is the channel length), so it can be assumed that the value of α_L is $0.1x$, $0.3x$ and $0.5x$, respectively (Pang, 2010).
3. The flow pattern is more complicated when all the wells are working and there will be water flowing through other parts of the reservoir outside the main flow paths (Koech, 2014). So not all tracer injected into DL-48B can be recovered in DL-48. Since the annual production of DL-48 accounts for approximately 15% of the total production in the area, it is assumed that the total tracer recovery in well DL-48 will be approximately 15% of that injected.

The distance between the injection and production wells DL-48B and DL-48 is 776 m, both the injection and the production rate are 30 kg/s during the period of domestic heating, which is 4 months of the year. According to Equation 3 and proposed assumptions, possible μ values and possible tracer concentration after 90 days can be calculated. Results are shown in Table 2 and Figures 6 and 7.

TABLE 2: Parameters of the simulated models for tracer recovery data with different dispersivity

Parameter	Simulation 1 $\alpha_L=76.7\text{m}$	Simulation 2 $\alpha_L=230.1\text{m}$	Simulation 3 $\alpha_L=383.5\text{m}$
Fluid velocity, μ (m/day)	1.04	0.43	0.29
$A\phi$ (m ²)	2600	6240	9460

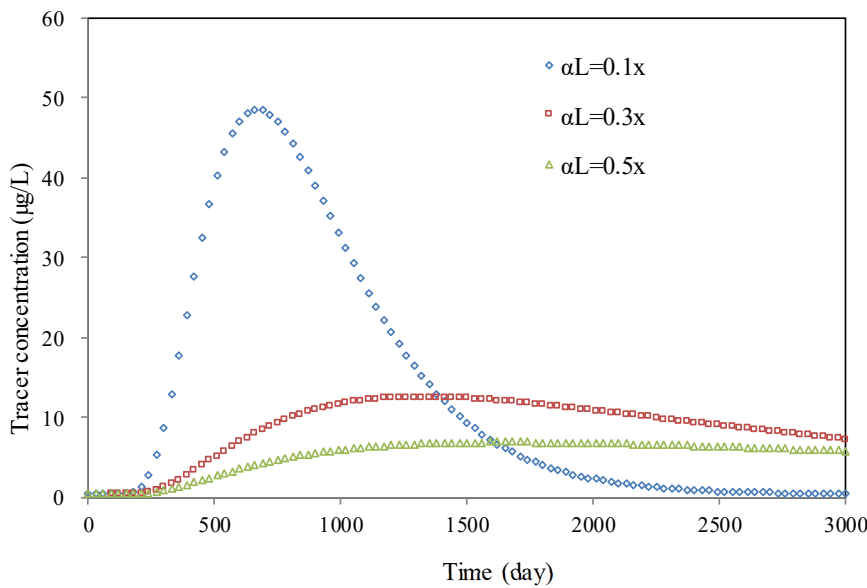


FIGURE 6: The results of the simulation of tracer recovery within 3000 days based on different dispersivity values

According to Figure 6, different dispersion coefficients give significantly different results. When the longitudinal dispersivity of the channel is 0.1 times the channel length, the breakthrough time is earlier and the peak concentration is much higher than in the other two cases. As Equation 3 shows, tracer breakthrough time depends on maximum fluid velocity and time of maximum concentration reflects the average fluid velocity. The width of the tracer pulse

normally reflects the flow path dispersion, and the tracer recovery is a function of time (Axelsson et al., 2005).

Figure 7 demonstrates tracer recovery within 250 days based on different dispersivity rates. After 150 days the tracer concentration has begun to increase. This explains why no recovery in the tracer test was seen after 90 days of sampling.

In comparison with hydraulic conductivity, which is 1.29 m/day in well DL-48B (Tian, 2014), and the fluid velocity μ shown in Table 2, the simulation which assumes a longitudinal dispersivity of 0.1 times the channel length seems to be much more reliable than the other two cases.

3.2 Cooling predictions

One of the main goals of a tracer test is to predict thermal breakthrough and temperature decline during long-term injection. The heat transfer between injection and production wells not only depends on the properties of the flow channels involved, but is also determined by the surface area and porosity of the flow channels. Therefore, it is important to have additional information on the flow path properties or geometry which is of geological or geophysical nature (Axelsson, 2013). Previous simulations of tracer recovery provide useful information about the cross-section that can be used for cooling predictions (Pang, 2010).

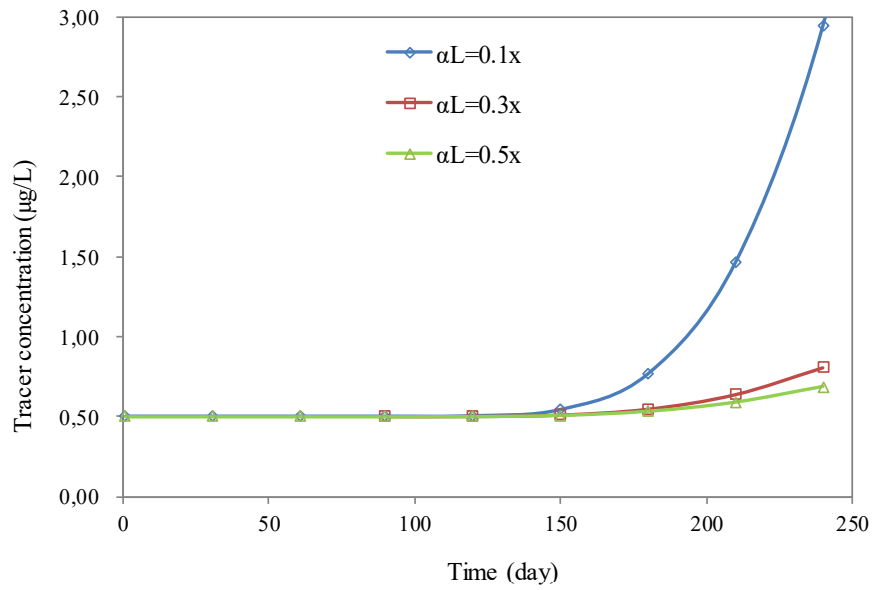


FIGURE 7: The results of the simulation of tracer recovery within 250 days based on different dispersivity values

3.2.1 Analytical model description

The model simulates a flow path along a fracture-zone, an interbed or permeable layer. Actually, it is a geometrically more restrained variant of the flow channel model described in Section 3.1.1. A detailed discussion of this model and the solution is provided in the paper by Axelsson et al. (2005). The mathematical equations giving the response of the model for cooling prediction are:

$$T(t) = T_0 - \frac{q}{Q}(T_0 - T_i) \left[1 - erf \left\{ \frac{kxh}{c_w q \sqrt{\kappa(t - \frac{x}{\beta})}} \right\} \right] \tag{4}$$

$$\beta = \frac{qc_w}{(\rho c)_f hb} \tag{5}$$

with

$$(\rho c)_f = \rho_w c_w \phi + \rho_r c_r (1 - \phi) \tag{6}$$

where $T(t)$ is the production fluid temperature, T_0 is the undisturbed reservoir temperature, T_i is the injection temperature, q and Q are rates of injection and production, respectively, erf is the error function, k is the thermal conductivity of the reservoir rock, κ is the thermal diffusivity of the reservoir rock, x is the distance between injection and production wells, ρ and c are density and heat capacity, respectively, with the indices w and r standing for “water” and “rock”.

3.2.2 Prediction of temperature change and propagation from injection well

The program Tracer (TR) part of the ICEBOX software was used to calculate the theoretical temperature decline for production well DL-48. Relevant parameters are discussed according to the hydrogeological information and development situation as follows and shown in Table 3:

- 1) During the heating season, the injection is 100% with a rate of 30 kg/s. While in other seasons, production rate is decreased due to lower demand. Thus, the average annual production rate is taken as 10 kg/s. Thus, 10 and 30 kg/s are both used to simulate the extreme cases for the cooling prediction.
- 2) Based on geological information, the Wumishan geothermal reservoir (Jxw) consists mostly of Mesoproterozoic dolomitic limestone. It is assumed, that thermal conductivity of the reservoir rock is 3.2 W/m K, density of the rock is 2677 kg/m³ and porosity of the reservoir 6% (Lin, 2006).
- 3) The flow channel length is 767 m, and cross-sectional area of the flow-channel $A\phi$ is assumed to be 4336 m² based on a dispersivity equalling 76.7 m. Considering the uncertainty of predictions, two extremes regarding different flow-channel dimensions were calculated. A pessimistic scenario was assumed, where the ratio between height (h) and width (b) of the flow channels was given by $h = 5 b$ and an optimistic scenario, where the ratio was given by $h = 20 b$.

TABLE 3: Model parameters used for the cooling predictions

Injection/production rate (kg/s)	Scenario	Flow channel distance (m)	Flow channel width b (m)	Flow channel height h (m)	Cross-section area (m ²)
30	Pessimistic	767	93.1	466	43400
	Optimistic		46.6	931	
10	Pessimistic	767	93.1	466	43400
	Optimistic		46.6	931	

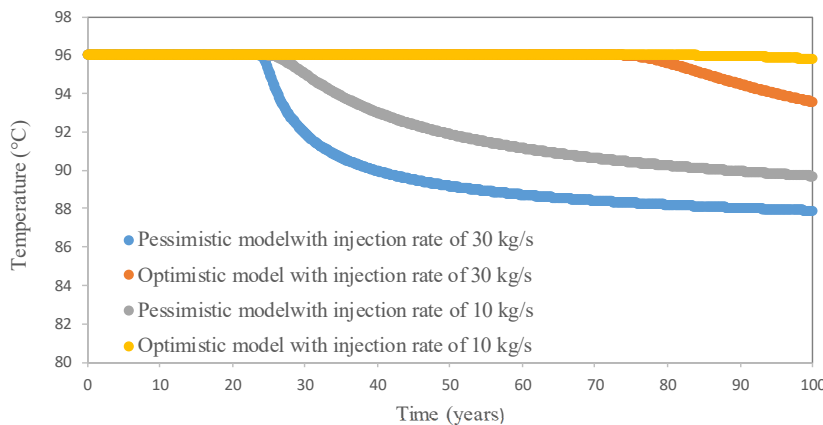


FIGURE 8: Cooling prediction for production well DL-48, with injection rates 10 and 30 kg/s, respectively, for 100 years

The cooling predictions (Figure 8) indicate that for an average annual production and injection rate of 10 kg/s, thermal breakthrough would occur in 80 years in case of a wide flow channel for an optimistic scenario and 27 years in case of a narrower flow channel for a pessimistic scenario. The cooling effect is relatively small for the optimistic model. Temperature stays nearly constant for the next 100 years, indicating no direct

connection between injection and production wells, while with the pessimistic model, the water in the production well cools down faster in the first 50 years with a temperature decline of 4°C.

With the highest production and injection rate of 30 kg/s, temperature drops faster and more rapidly compared to the lower injection rate of 10 kg/s. Thermal breakthrough would occur in 72 years in case of a wide flow channel for an optimistic scenario and in 24 years in case of a narrower flow channel for a pessimistic scenario. Temperature in the production well decreases faster in the first 50 years with declines of 6.8°C in the more pessimistic case. If the injection rate increases, the thermal breakthrough time will be earlier and the influence on cooling will become higher. Hence, it is recommended to keep the injection rate as it is.

It is important to note that the production rate always decreases after the heating period because of lower demand of geothermal energy which is beneficial for temperature recovery. This means that the cooling influence will be smaller than the model predicted.

4. NUMERICAL MODELLING

4.1 Background of numerical modelling with MODFLOW

MODFLOW is a FORTRAN program developed by the United States Geological Survey (USGS), which can simulate groundwater flow and levels under complex hydrogeological conditions with various hydrological processes and is widely used in regulatory situations (Jang et al., 2016).

The equation governing groundwater flow through saturated porous media in three dimensions is derived from Darcy's law and the continuity equation, and is given as (Harbaugh et al., 2000):

$$\frac{\partial}{\partial x} \left(K_{xx} \frac{\partial h}{\partial x} \right) + \frac{\partial}{\partial y} \left(K_{yy} \frac{\partial h}{\partial y} \right) + \frac{\partial}{\partial z} \left(K_{zz} \frac{\partial h}{\partial z} \right) + W = S_s \frac{\partial h}{\partial t} \quad (7)$$

where K_{xx} , K_{yy} and K_{zz} are the hydraulic conductivities (m/d) along the x, y, and z axes that are assumed to be parallel to the principal axes of the hydraulic conductivity tensor, h is the hydraulic head (m), W is the volumetric flux per unit volume representing sources and/or sinks of water (1/d), S_s is the specific storage of the material (1/m) and t is time (d). Here, K_{xx} , K_{yy} and K_{zz} are the functions of space (x , y , z) and W is a function of space and time (t).

In this study, the Visual MODFLOW Flex (2015.1) software has been used for simulating the groundwater dynamics. This version includes the simulation of saturated-unsaturated flow processes, density dependent flow processes, parameter optimization processes and solute transport processes (Zhou and Li, 2011). A finite difference grid was used and MODFLOW 2000 was chosen as an engine to run a transient state numerical model from 26th August, 2013 to 26th August, 2015. Two additional packages were used in this project:

- 1) MT3DMS: Visual MODFLOW Flex supports MT3DMS v.5.2. MT3DMS is a transport model for simulating advection, dispersion, and chemical reactions of contaminants in groundwater flow systems. This package was used to model the concentration of the observation wells after tracer injection (Zheng and Wang, 1999).
- 2) PEST: An effective tool of automating parameter estimation, calibration and sensitivity analysis, it allows running parameter estimation using results from both groundwater flow and contaminant transport simulations (Doherty et al., 2010).

4.2 Numerical reservoir modelling and calibration

4.2.1 Conceptual model

The Jxw geothermal reservoir in the Dongli Lake area is an extensive, low-temperature geothermal system hosted mainly by Mesoproterozoic dolomitic limestone. It belongs to semi-opened and semi-closed bedrock subsystems, where the geothermal karst fluids exist (Ruan, 2011). Considering that most of the wells are distributed on the western side of the Cangdong fault, a small area with intensive production and injection wells was chosen for the conceptual and numerical modelling (Figure 3).

In order to create a conceptual model, the study area was vertically divided into four layers. Based on borehole geology, a 3D structural model was created (Figure 9). Hence, layer 1 is the Quaternary porous formation. Layer 2 includes Cenozoic Minghuazhen Group (Nm) and Guantao Group (Ng). Layer 3 is the karstic-fracture geothermal reservoir, including Paleozoic Ordovician (O) and Cambrian (€). Layer 4 which is the main study reservoir consists of the Mesoproterozoic Jixian Wumishan Group (Jxw).

From pumping test results of the wells in this area (Tian, 2014), hydraulic conductivity of the reservoir is between 0.59 m/d and 3.3 m/d with permeability between 4.89×10^{-13} and 1.25×10^{-13} m². Porosity is around 5-6%, and the thickness of the reservoir is from 1050 to 2250 m.

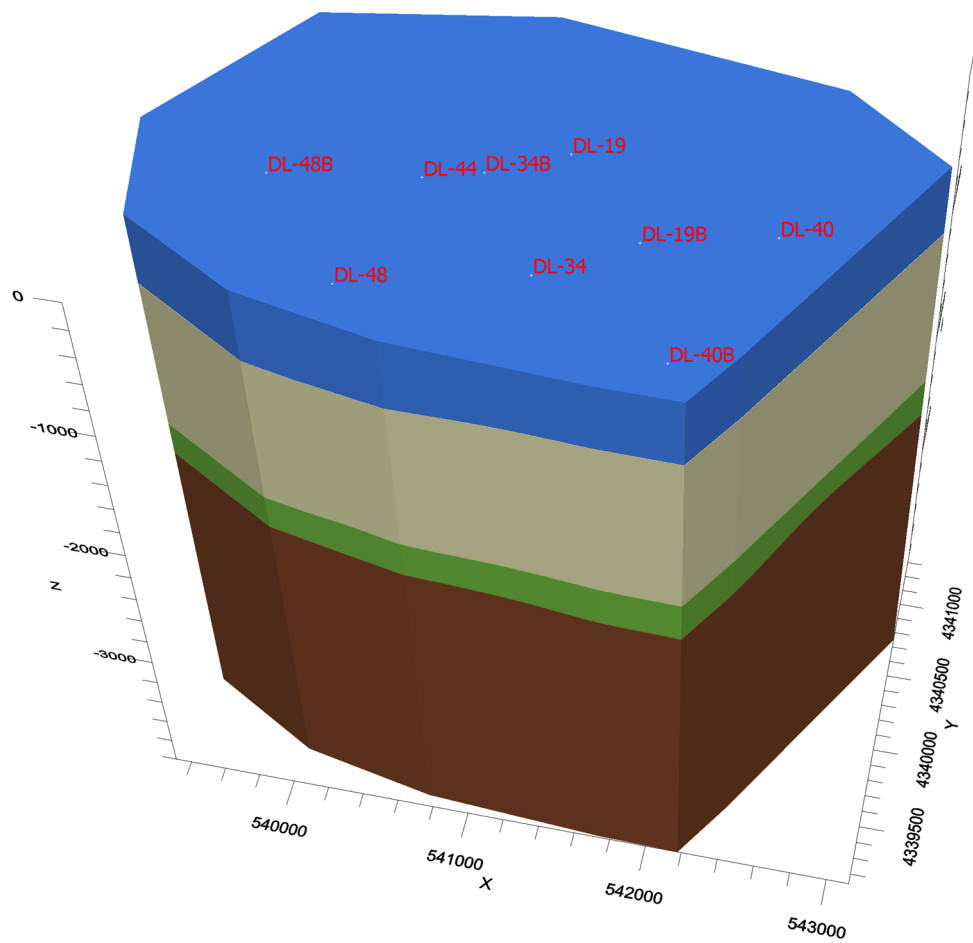


FIGURE 9: The 3D model of the Jxw geothermal reservoir

4.2.2 Numerical model

A finite difference grid was used for numerical modelling. Each layer of the conceptual model was discretized horizontally into a grid of 100×120 cells with cell height of 22.13 m and cell width of 31.78 m. For more accurate simulation of the water levels and tracer concentration between the injection and production well, a grid around well DL-48 and DL-48B was refined by a factor of two (Figure 10).

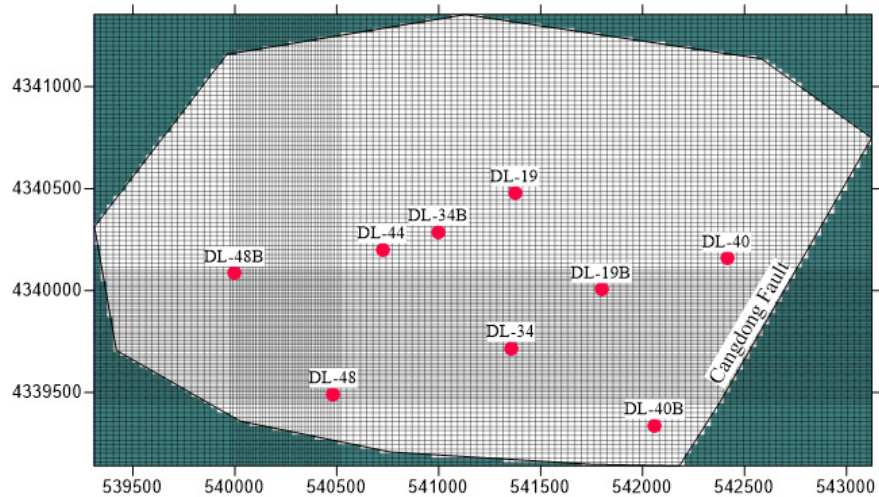


FIGURE 10: Numerical model grid

Based on the information of the deepest well with depth of 4040 m in this area, the reservoir below 4000 m depth is poorly developed with pores and fissures. Consequently, the bottom boundary was considered as no-flow boundary.

The flow direction is mainly from northwest to southeast according to the initial water level contours and the inflow and outflow flux of each boundary can be calculated by Darcy's Law. The specified flux boundary was used with these fluxes in the model and a small adjustment was made during the process of calibration. Horizontal hydraulic conductivity $K_{x,y}$, vertical hydraulic conductivity (K_z) and storativity (S_s) were defined as 1.2 m/d, 0.12 m/d and $1 \times 10^{-5} \text{ m}^{-1}$, respectively, in layer 4 (the main reservoir).

After all hydrogeological parameters were implemented into the numerical model, MODFLOW 2000 was used to run numerical engines and simulate groundwater level changes in the reservoir. Where observation data was available (from DL-19, DL-40, DL-44, DL-48), it was possible to evaluate how reliable the numerical model is. Therefore, calculated water levels are plotted against observed levels. In the perfect case scenario, there is a linear relationship between the calculated and observed heads. After a first MODFLOW 2000 run, the deviation was too high (Figure 11). Most calculated water levels are higher than the observed values, and both the absolute residual mean (ARM) and the root mean square error (RMSE) are very high, 6.14 m and 13.24 m, respectively. Thus the input parameters (hydrogeological parameters) had to be adjusted.

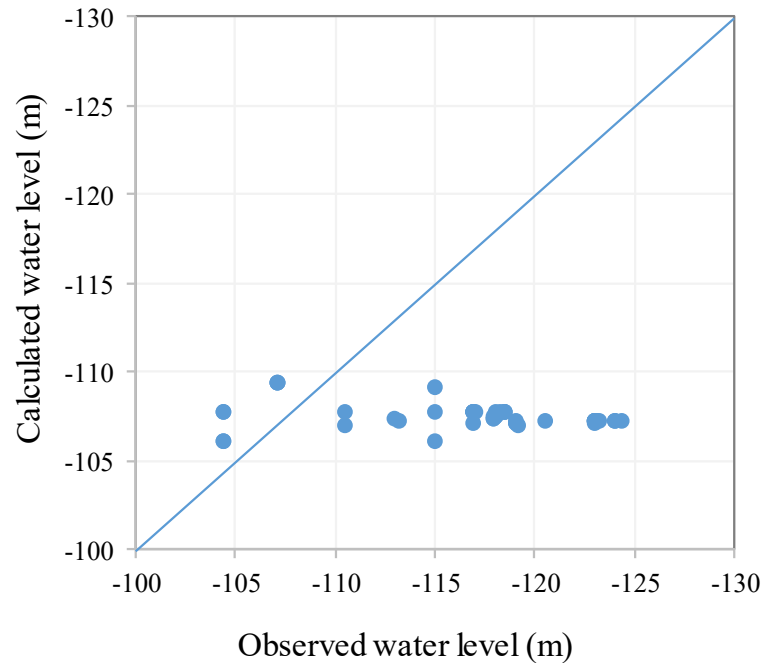


FIGURE 11: The fitting of the observed water levels and simulated water levels before calibration

Hydrogeological parameters of layer 4 (main reservoir) were manually adjusted until acceptable fit between observed and simulated water levels was reached. After manual calibration $K_{x,y}$ was 1 m/d, K_z was 0.1 m/d and S_s was $5 \times 10^{-6} \text{ m}^{-1}$ in layer 4.

In order to increase the accuracy of the model, an automatic parameter estimation tool (PEST) was used to minimize errors between the observed and simulated data. This was also used to estimate the distribution of reservoir parameters. Pilot points were placed and fixed in the wells with known $K_{x,y}$, which were obtained from pumping test data reported by Tian (2014) (Table 4). Additional pilot points were then added scattered over the study area. $K_{x,y}$, K_z and S_s in layer 4 were constrained in the range of 0.1-10 m/d, 0.01-1 m/d and 1×10^{-7} - $1 \times 10^{-4} \text{ 1/m}$, respectively. This resulted in 15 pilot points with 3 types of parameters to be calibrated. The spatial hydraulic conductivity and storativity fields were derived by interpolation among pilot points using kriging variograms (Woodward et al., 2016).

TABLE 4: The hydraulic conductivity of fixed pilot points from well test data

Well	Hydraulic conductivity (m/d)	Well	Hydraulic conductivity (m/d)
DL-40B	2.85	DL-40	1.03
DL-48	3.3	DL-34	0.85
DL-19B	1.38	DL-44	0.77
DL-48B	1.29	DL-44B	0.73

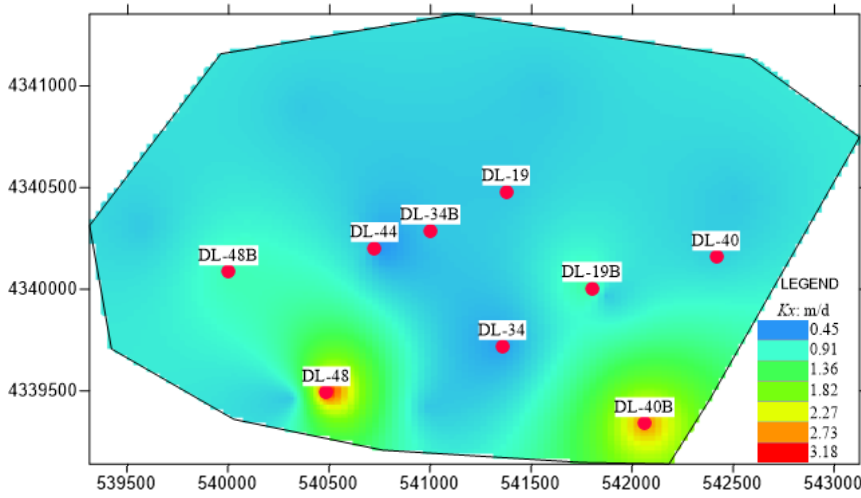


FIGURE 12: A map of simulated hydraulic conductivity ($K_{x,y}$) in the Jxw reservoir after model calibration

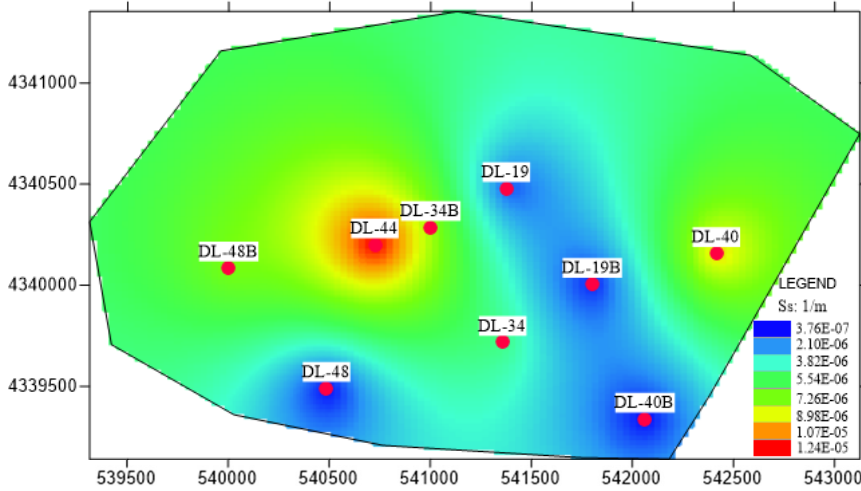
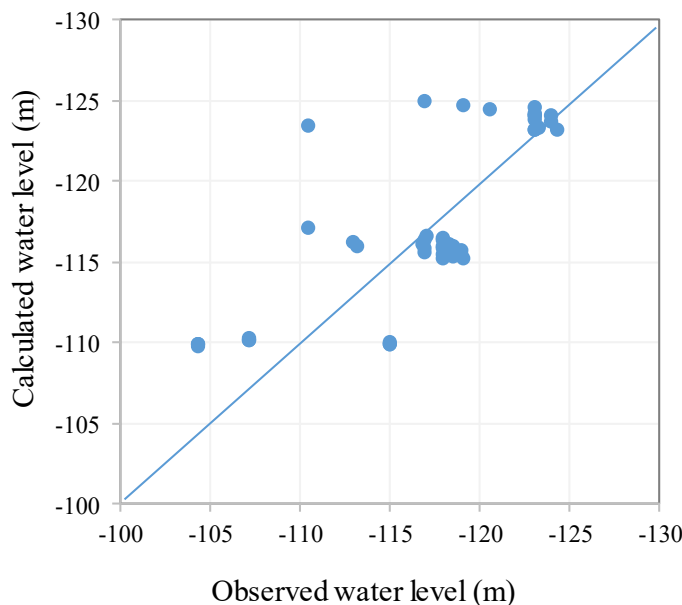


FIGURE 13: A map of simulated storativity in the Jxw reservoir (S_s) after model calibration



After running PEST, a new distribution of parameters was received and they were applied to the new model. Figures 12 and 13 show the distribution of $K_{x,y}$ and S_s used in the model after calibration. The range of $K_{x,y}$, K_z and S_s in layer 4 is mostly between 0.45 and 3.18 m/day, 0.05 and 0.33 m/day and 2.09×10^{-6} - $1.24 \times 10^{-5} \text{ m}^{-1}$, respectively, which can be reflected better by the heterogeneity of the reservoir rather than a zonal approach.

The final calibrated model produced reasonable agreement between the simulated and observed water levels at the calibration targets (Figure 14). The absolute residual mean (ARM) was 2.94 m, while the root mean square error (RMSE) was 3.84 m. For a model with an area of 6.32 km² a standard error estimate of 0.57 m and correlation coefficient of 0.77 were considered to be acceptable. Comparing to the model before the PEST running, both the parameter distributions and water levels are closer to the actual situation.

FIGURE 14: The fitting of the observed water levels and simulated water levels in the Jxw reservoir after PEST

4.3 Prediction of tracer concentration in the production well

The MT3DMS numerical engine was used to estimate the recovery time and the tracer concentration in the production wells. For further modelling, it was assumed that the tracer is conservative and no adsorption or desorption occurs in the reservoir, only convection and dispersion were considered. Hydraulic conductivity and storativity were deduced from the groundwater flow model. Total porosity was used to determine the chemical reaction coefficients and for calculating the average linear groundwater flow velocity (Waterloo Hydrogeologic, 2015). The longitudinal dispersivity was set the same as in the analytical method, i.e. 76.7, 230.1 and 383.5 m for the three different simulation scenarios.

The injection of tracers was set on the first day of injection with a maximum dissolved concentration of $3 \times 10^8 \mu\text{g/L}$. There are two different boundary conditions that can be used in this software, well boundary condition and constant concentration boundary condition. For the first one, tracer concentration was set at the injection well, but the concentration was diluted quickly to be $1.26 \times 10^7 \mu\text{g/L}$ after one day of injection. While, for the other one, the grid cell with the injection well was set to have a constant concentration of $3 \times 10^8 \mu\text{g/L}$ during the first day of injecting water. This difference also affected the results of tracer recovery concentration, as shown in Table 5. It can be seen that the recovery time is the same in both of these cases, but the concentration is almost one order of magnitude smaller when setting a well boundary condition compared to when setting a constant concentration.

TABLE 5: Recovery time and corresponding concentration of production well with two methods

Scenarios	Recovery time (years)	Concentration of well DL-48 ($\mu\text{g/L}$)		
		$\alpha_L=76.7 \text{ m}$	$\alpha_L=230.1 \text{ m}$	$\alpha_L=383.5 \text{ m}$
Tracer injected with well	1.1			2.51×10^{-31}
	2.1		4.26×10^{-30}	3.57×10^{-21}
	5.3	3.14×10^{-32}	2.01×10^{-14}	1.47×10^{-8}
	9.7	1.33×10^{-21}	4.68×10^{-8}	4.63×10^{-4}
Tracer as constant concentration	1.1			1.68×10^{-30}
	2.1		5.78×10^{-29}	3.60×10^{-20}
	5.3	4.96×10^{-31}	1.87×10^{-13}	1.74×10^{-7}
	9.7	6.05×10^{-21}	3.44×10^{-7}	4.24×10^{-3}

We can also notice that the tracer concentration was diluted very quickly and it moved very slowly. For the most pessimistic case ($\alpha_L=384 \text{ m}$), it takes the tracer more than a year to arrive at the production well, with very small concentration which is below the detection limit. Even at the end of 10 years, the concentration is still below detection limit (Figure 15). This means that more than 10 years are needed to get recovery with the tracer testing.

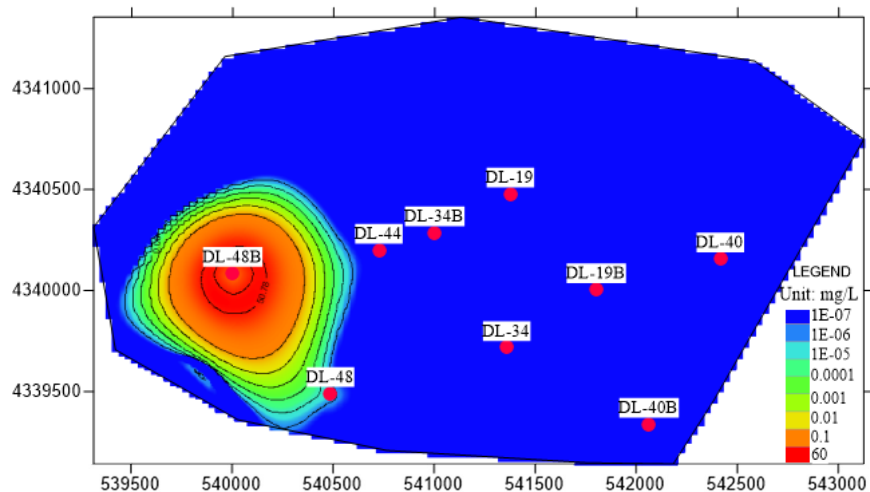


FIGURE 15: Tracer concentration contours in the Jxw reservoir after 10 years ($\alpha_L=384 \text{ m}$)

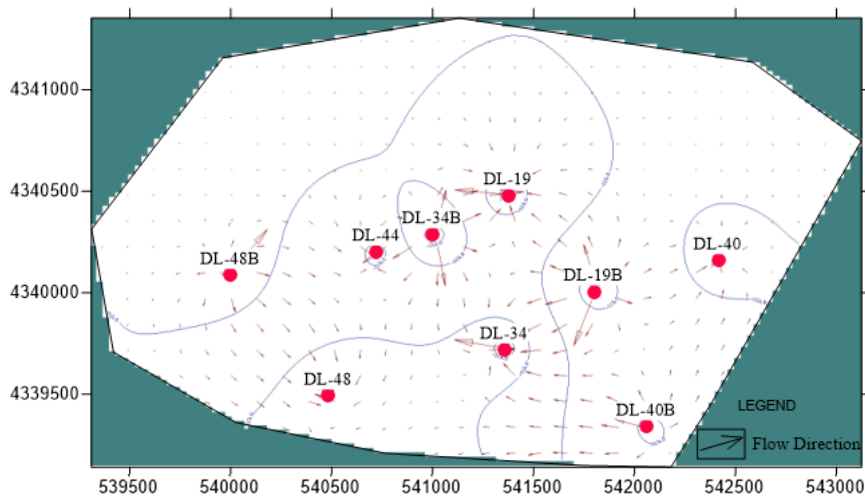


FIGURE 16: Flow directions during production and injection periods (day 127, scale factor 0.4)

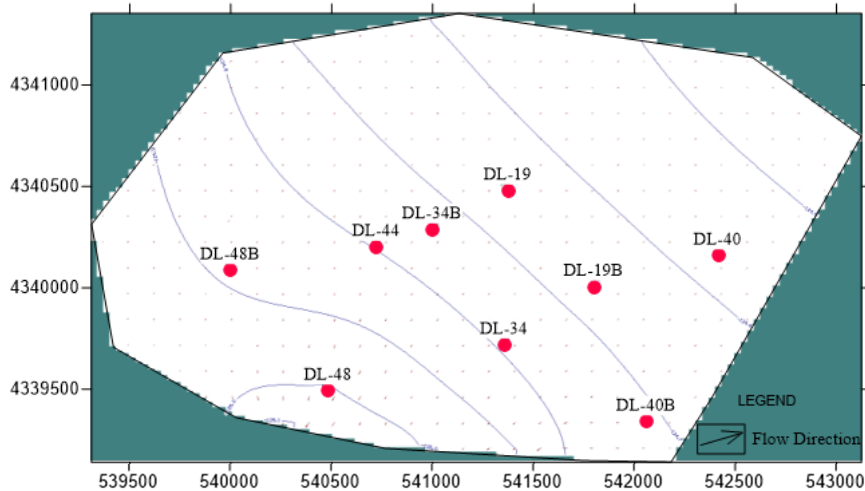


FIGURE 17: Flow directions without production and injection (day 730, scale factor 0.4)

From the flow directions, which also show velocities of the water flow at different times (Figures 16 and 17), we can find that production and injection change the flow pattern around the wells compared to other times. However, the volume of the reservoir is so big and injection or production influential radius are rather small. The flow is relatively slow with the biggest rate of 0.12 m/d around wells, while in other place and at other times this value is only around 0.01 m/d. Compared with the analytical model, this velocity only accounts for 3.4% of simulation 3 (0.29 m/d), which also explains why the tracer needs such a long time to arrive at the production well. Results show that there is no direct connection between the production and injection wells and neither model predicts cooling in the next 24 years.

5. DISCUSSION

Tracer testing in the Wumishan (Jxw) geothermal reservoir in the Dongli Lake area of Tianjin has been interpreted with respect to concentration change and cooling of the production well, using both an analytical and a complex numerical method. The analytical method, with the assumption that recovery would appear after 90 days, showed that thermal breakthrough would occur after 80 years for an optimistic scenario (narrow flow channel) and after 27 years for a pessimistic scenario (wide flow channel) assuming an average annual production and injection rate of 10 kg/s.

Although the heat transfer was not simulated with the numerical model, information was received from the tracer concentration prediction. The results show that when the longitudinal dispersivity is 384 m, the recovery time is more than 10 years. As thermal changes are known to be extremely slow, compared to pressure and chemical changes, due to the thermal inertia of the rock formation involved (Axelsson, 2012b), hence the thermal breakthrough time is estimated to be much longer than 10 years. Thus, these two different models show that there is no direct connection between the production and injection wells, which also explains why no tracer recovery was observed in the samples.

The analytical method assumes that the flow paths are directly from the injection point to the pumping wells and the influence of a regional gradient is not taken into account (Haerens, 1999). It provides a simple and effective way to interpret tracer testing results. While a numerical model can better reflect the reservoir conditions and flow patterns and thus provide better results, but it takes longer to implement data and make a run. The results depend heavily on the reliability of the model, which is why the model should be calibrated with enough observation data. If the model is considered to fit well with the observation data, it can be used for cooling prediction and consequently play an important role in the reservoir management.

6. CONCLUSIONS AND RECOMMENDATIONS

The Wumishan (Jxw) geothermal reservoir in the Dongli Lake area is an extensive, low-temperature geothermal system hosted mainly by Mesoproterozoic dolomitic limestone. It belongs to semi-open and semi-closed bedrock subsystems, where geothermal karst fluids exist. The heat source of the reservoir is presumably in the upper mantle and radioactive decay in granite (at about 8-16 km depth). The origin of the water is meteoric from ancient times. The Quaternary and Tertiary formations consist of clay and sandstone, forming a good caprock for the geothermal reservoir. The Cangdong fault is a major fault which can conduct heat from the bottom of the reservoir to the shallow part by heat convection.

In order to study the flow paths and predict the cooling due to long term injection, tracer tests were performed. To interpret the tracer tests quantitatively, both an analytical method, developed by ÍSOR (Iceland Geosurvey), and a numerical method using the Visual MODFLOW flex software were applied and discussed in the report.

For the analytical model, it was assumed that the recovery was very slow and would appear after 90 days. For the three cases of longitudinal dispersivity, 77, 230 and 384 m, the tracer concentration began to increase after 150 days. The breakthrough time was earlier and the peak concentration was much higher, with a longitudinal dispersivity of 76.7 m or 0.1 times the channel length, than for the other two cases where the longitudinal dispersivity is higher, or 0.3 times and 0.5 times the channel length. When the dispersivity was 76.7 m, thermal breakthrough would occur after 80 years for an optimistic scenario (narrow flow channel) and after 27 years for a pessimistic scenario (wide flow channel) for average annual production and injection rates of 10 kg/s.

A numerical reservoir model was developed for the Dongli Lake geothermal area. It covers an area of 6.32 km². An automatic parameter estimation tool (PEST) was used to minimize errors between observed and simulated heads and to estimate the distribution of reservoir parameters. After calibration, the range of hydraulic conductivity ($K_{x,y}$, K_z) and storativity (S_s) in the Jxw reservoir were found to be in the range 0.45-3.18 m/day, 0.05-0.33 m/day and 2.09×10^{-6} - 1.24×10^{-5} m⁻¹, respectively. This better reflects the heterogeneity of the reservoir than a zonal approach, where it is assumed that these parameters are constant within the zones. The final calibrated model produced reasonable agreement between the simulated and observed water levels and was applied to predict the tracer concentration in the production well.

For the most pessimistic case of a longitudinal dispersivity of 384 m, the tracer will take more than a year to arrive at the production well, according to the model, with very small concentration, outside the detection limit. Results show that there is no direct connection between production and injection wells and neither model predicts cooling in the next 24 years. Based on the results of this study, some recommendations are put forward:

- 1) A numerical model is helpful when designing tracer tests. It can be used to estimate the minimum quantity of tracer required, the breakthrough time and the peak arrival time. In the meantime, tracer tests data can also help to improve the calibration of a numerical model, which, in turn, could provide more information about the flow paths.

- 2) In this case study, sampling is suggested to be continued over the next one to two years at a low sampling frequency. More information should be collected to improve the numerical model.
- 3) SEAWAT software (Langevin et al., 2008) is suggested to be used to predict the cooling of the production well. It is a computer program intended to simulate multi-species solute and heat transport which couples MODFLOW-2000 with MT3DMS. Heat transport calculations with SEAWAT are based on the analogy between solute and heat transport (Vanderbohede et al., 2011) with the temperature being treated as one of the species.

ACKNOWLEDGEMENTS

I would like to thank the United Nation University for supporting me to accomplish this training programme. Thanks to Mr. Lúdvík S. Georgsson, director, as well as to all the technical staff of UNU-GTP, Mr. Ingimar G. Haraldsson, Ms. Málfríður Ómarsdóttir, Ms. Thórhildur Ísberg and Mr. Markús A. G. Wilde, for giving me a family feeling in Iceland.

Sincere thanks to Dr. Gudni Axelsson and Ms. Saeunn Halldórsdóttir, from ÍSOR, for the supervision and guidance during the preparation of the present project. I would like to express the deepest and sincerest gratitude to my supervisors, Ms. Vaiva Čypaitė and Ms. Valdís Guðmundsdóttir. Thanks for providing me with patient guidance and advice, and sharing knowledge and experience, thanks for all the help and assistance.

Thanks to my colleagues of the Institute of Hydrogeology and Environmental Geology (IHEG) staff members, especially to Mr. Wang Guiling, Mr. Lin Wenjing, Mr. Lu Chuan, Mr. Liu Feng, for their support given during the training in Iceland. Thanks for the support given by Tianjin Geothermal Exploration and Development Designing Institute for allowing the use of the data for the purpose of the present work.

Thanks to the other UNU Fellows for their support and friendship over the last six months.

Finally, I would like to express my deepest appreciation to my family. Thanks to my husband and my son for their support.

REFERENCES

- Alramadhan, A.A., Kilicaslan, U., and Schechter, D.S., 2015: Analysis, interpretation, and design of inter-well tracer tests in naturally fractured reservoirs. *J. Petroleum Science Research*, 4-2, 97-122.
- An Q.S., Wang Y., Zhao J., Luo C., and Wang Y., 2016: Direct utilization status and power generation potential of low-medium temperature hydrothermal geothermal resources in Tianjin, China: a review. *Geothermics*, 64, 426-438.
- Axelsson, G., 2012a: Role and management of geothermal reinjection. *Presented at "Short course on geothermal development and geothermal wells"*, organized by UNU-GTP and LaGeo, Santa Tecla, El Salvador, UNU-GTP SC-14, 21 pp.
- Axelsson, G., 2012b: The physics of geothermal energy. In: Sayigh, A., (ed.), *Comprehensive renewable energy*. Elsevier, Oxford, 3–50.
- Axelsson, G. 2013: *Tracer tests in geothermal resource management*. *EPJ Web of Conferences*, EDP Sciences, 50, 8 pp.

Axelsson, G., Björnsson, G., and Montalvo, F., 2005: Quantitative interpretation of tracer test data. *Proceedings of the World Geothermal Congress 2005, Antalya, Turkey*, 12 pp.

Axelsson, G., and Dong Z., 1998: The Tanggu geothermal reservoir (Tianjin China). *Geothermics*, 27, 271–294.

Cheng, W., Tedesco, D., and Poreda, R., 2008: The Tianjin geothermal field (north-eastern China): water chemistry and possible reservoir permeability reduction phenomena. *Geothermics*, 37, 400–428.

Diaz, A.R., Kaya, E., and Zarrouk, S.J., 2016: Reinjection in geothermal fields - A worldwide review update. *Renewable and Sustainable Energy Reviews*, 53, 105-162.

Doherty, J.E., Hunt, R.J., and Tonkin, M.J., 2010: *Approaches to highly parameterized inversion: A guide to using PEST for model-parameter and predictive-uncertainty analysis*. US Geological Survey Scientific Investigations, report 2010-5211, 71 pp.

Duan Z., Pang Z., and Wang X., 2011: Sustainability evaluation of limestone geothermal reservoirs with extended production histories in Beijing and Tianjin, China. *Geothermics*, 40, 125–135.

Fan Y., 2006: *A study of the storage capacity of geothermal reservoirs and the exploitation dynamics of thermal water in Tianjin* (in Chinese). China University of Geosciences, Beijing, MSc thesis, 66 pp.

Haerens, B., Brouyere, S., and Dassargues, A., 1999: Detailed calibration of a deterministic transport model on multi-tracer tests: analysis and comparison with semi-analytical solutions. *Proceedings of Model CARE 99: Calibration and Reliability in Groundwater Modelling, ETH, Zurich, Switzerland*, 6 pp, website: hdl.handle.net/2268/2560.

Harbaugh, A.W., Banta, E.R., Hill, M.C., and McDonald, M.G., 2000: *MODFLOW-2000, the US Geological Survey modular ground-water model – user guide to modularization concepts and the ground-water flow process*. US Geological Survey, open-file report 00-92, Reston, VA, 121 pp.

Jang C., Chen C., Liang C., and Chen J., 2016: Combining groundwater quality analysis and a numerical flow simulation for spatially establishing utilization strategies for groundwater and surface water in the Pingtung Plain. *J. Hydrology*, 533, 541-556.

Koech, V.K., 2014: *Numerical geothermal reservoir modelling and infield reinjection design, constrained by tracer test data: case study for the Olkaria geothermal field in Kenya*. University of Iceland, MSc Thesis, UNU-GTP, report 5, 80 pp.

Langevin, C.D., Thorne Jr., D.T., Dausman, A.M., Sukop, M.C., and Guo, W., 2008: *SEAWAT vs.4: a computer program for simulation of multi-species solute and heat transport*. US Geological Survey techniques and methods, Book 6, Chapter A22, 39 pp.

Leblanc, D.R., Garabedian, S.P., Hess, K.M., Gelhar, L.W., Quadri, R.D., Stollenwerk, K.G., and Wood, W.W., 1991: Large-scale natural gradient tracer test in sand and gravel, Cape Cod, Massachusetts. *Water Resources Research*, 27, 895-910.

Lin L., 2006: *Sustainable development and utilization of thermal groundwater resources in the geothermal reservoir of the Wumishan Group* (in Chinese). China University of Geosciences, Beijing, PhD thesis, 133 pp.

Minissale, A., Borrini, D., Montegrossi, G., Orlando A., and Tassi, F., 2008: The Tianjin geothermal field (north-eastern China): Water chemistry and possible reservoir permeability reduction phenomena. *Geothermics*, 37, 400-428.

- Mondejar, G.C., 2012: Hydrological flow and thermal interference modelling in the Mahanagdong geothermal field, Philippines, using four types of Naphthalene disulfonate tracer. Report 22 in: *Geothermal training in Iceland 2010*. UNU-GTP, Iceland, 467-500.
- Nottebohm, M., Licha, T., and Sauter, M., 2012: Tracer design for tracking thermal fronts in geothermal reservoirs. *Geothermics*, 43, 37-44.
- Pang J., 2010: Reinjection into well ST0902 and tracer testing in the Xiongxiang geothermal field, Hebei Province, China. Report 25 in: *Geothermal training in Iceland 2010*. UNU-GTP, Iceland, 493-524.
- Ruan C., 2011: Numerical modelling of water level changes in Tianjin low-temperature geothermal system, China. Report 31 in: *Geothermal training in Iceland 2011*. UNU-GTP, Iceland, 775-798.
- Ruan C., Sun B., Shen J., Gao X., and Liu R., 2015: The injection research of Dongli Lake bedrock reservoir in Binhai New Area. *Proceedings of the World Geothermal Congress 2015, Melbourne, Australia*, 9 pp.
- Tian G., 2014: *Sustainable development and utilization of geothermal resources in the Donglihu resort in Tianjin* (in Chinese). China University of Geosciences, Beijing, MSc thesis, 106 pp.
- Vandenbohede, A., Hermans, T., Nguyen, F., and Lebbe, L., 2011: Shallow heat injection and storage experiment: Heat transport simulation and sensitivity analysis. *J. Hydrology*, 409, 262-272.
- Waterloo Hydrogeologic, 2015: *Visual MODFLOW Flex user manual*. Waterloo Hydrogeologic, software, 569 pp.
- Woodward, S.J.R, Wöhling, T., and Stenger, R., 2016: Uncertainty in the modelling of spatial and temporal patterns of shallow groundwater flow paths: The role of geological and hydrological site information. *J. Hydrology*, 534, 680-694.
- Zhao N., 2010: Geochemical simulation of lake water injection into the geothermal reservoir in Tianjin, China. Report 32 in: *Geothermal training in Iceland 2010*. UNU-GTP, Iceland, 711-730.
- Zheng C., and Wang P.P., 1999: *MT3DMS: A modular three-dimensional multispecies model for simulation of advection, dispersion and chemical reactions of contaminants in groundwater systems: Documentation and user's guide*. US Army Engineer Research and Development Center, Vicksburg, MI, contract report SERDP-99-1, 239 pp.
- Zhou Y., and Li W., 2011. A review of regional groundwater flow modelling. *Geoscience Frontiers*, 2-2, 205-214.